lncRNA-MALAT1 promotes high glucose-induced H9C2 cardiomyocyte pyroptosis by downregulating miR-141-3p expression

AISHAN WU[1], WEILI SUN[2] and FENGYING MOU[3]

Departments of [1]Cardiology II and [2]Anesthesiology, Weihai Municipal Hospital, Weihai, Shandong 264200; [3]Department of Ultrasound, Weifang People's Hospital, Weifang, Shandong 261041, P.R. China

Received August 8, 2020; Accepted December 3, 2020

DOI: 10.3892/mmr.2021.11898

Abstract. Diabetic cardiomyopathy (DCM) is caused by diabetes and can result in heart failure. Long non-coding RNAs (lncRNAs) have been demonstrated to be closely associated with DCM development. The present study aimed to investigate whether lncRNA-metastasis-associated lung adenocarcinoma transcript-1 (MALAT1) altered high glucose (HG)-induced H9C2 cardiomyocyte pyroptosis by targeting microRNA (miR)-141-3p. H9C2 cells were treated with normal glucose (NG) or HG. lncRNA-MALAT1 and miR-141-3p expression levels were determined via reverse transcription-quantitative PCR (RT-qPCR). MALAT1 and miR-141-3p knockdown and overexpression were established and confirmed via RT-qPCR. The association between MALAT1 expression and miR-141-3p expression, as well as the induction of pyroptosis and gasdermin D (GSDMD)-N expression were evaluated by performing dual luciferase reporter, TUNEL staining and immunofluorescence staining assays, respectively. Western blotting was conducted to measure the expression levels of pyroptosis-associated proteins, including apoptosis-associated speck-like protein, GSDMD-N, caspase-1, nucleotide oligomerization domain-like receptor protein 3 and GSDMD. MALAT1 mRNA expression levels were significantly increased, whereas miR-141-3p expression levels were significantly decreased in HG-treated H9C2 cells compared with the NG group. Compared with the HG group, MALAT1 overexpression significantly reduced miR-141-3p expression levels, increased the rate of TUNEL positive cells and upregulated the expression levels of pyroptosis-associated proteins. MALAT1 knockdown displayed the opposite effect on the rate of TUNEL positive cells and the expression levels of pyroptosis-associated proteins. Furthermore, the rate of TUNEL positive cells, and GSDMD-N and pyroptosis-associated protein expression levels were significantly reduced by miR-141-3p overexpression in MALAT1-overexpression H9C2 cells. The results indicated that compared with NG treatment, HG treatment increased MALAT1 expression levels and decreased miR-141-3p expression levels in H9C2 cells. Therefore, the present study suggested that lncRNA-MALAT1 targeted miR-141-3p to promote HG-induced H9C2 cardiomyocyte pyroptosis.

Correspondence to: Ms. Fengying Mou, Department of Ultrasound, Weifang People's Hospital, 151 Guangwen, Kuiwen, Weifang, Shandong 261041, P.R. China
E-mail: haoqxs@yeah.net

Key words: long non-coding RNA-metastasis-associated lung adenocarcinoma transcript-1, microRNA-141-3p, H9C2, cardiomyocytes, pyroptosis, high glucose

Introduction

Diabetic cardiomyopathy (DCM) is a cardiovascular complication of diabetes that is one of the primary causes of disability or death in patients with diabetes worldwide (1). Myocardial cell and fibroblast death are fundamental alterations in DCM, which can trigger heart remodeling and lead to left ventricular dysfunction, resulting in the occurrence of DCM and heart failure (2). The abnormal glucose metabolism caused by high glucose (HG) is a key initiating factor of DCM (3). As the disease progresses, oxidative stress damage of the myocardial tissue is increased, and excessive active oxygen increases the expression levels of various inflammatory factors and induces the inflammatory response (4). The long-term inflammatory environment induces tissue and cell damage (4). However, the exact mechanism underlying DCM is not completely understood. Recent progress in the field of diabetes research has suggested that pyroptosis may be closely associated with the disease (5).

Pyroptosis is essential in the development of organs, cell renewal, differentiation and other physiological processes (6). Pyroptosis requires nucleotide oligomerization domain-like receptor protein (NLRP)3 to recognize pathogen-associated molecules and damage-associated molecules to induce caspase-1 and caspase-4/5/11 expression (7,8). Caspase expression results in cleavage of the downstream gasdermin D (GSDMD) protein, leading to cell membrane rupture, and the release of cell contents and inflammatory factors, including IL-1 and IL-18 (7,8). The production of inflammasomes, which contain large multiprotein complexes

consisting of caspase-1, apoptosis-associated speck-like protein (ASC) and NLRP, in cardiac fibroblasts is indispensable (9).

The field of epigenetics has gradually become a research hotspot for the investigation of various diseases, and its subcategories primarily involve the fields of microRNAs (miRNAs/miRs), long non-coding RNAs (lncRNAs) and DNA methylation (10,11). Recently, Zhang *et al* (12) reported that metastasis-associated lung adenocarcinoma transcript-1 (MALAT1) expression was increased significantly in heart tissues derived from diabetic model rats, whereas MALAT1 knockdown enhanced left ventricular function by reducing cardiomyocyte apoptosis. MALAT1 was originally reported to be overexpressed in tumor tissue samples, and to participate in the regulation of tumor cell proliferation, invasion, migration and metabolism (13). Further research on lncRNAs and vascular diseases by Michalik *et al* (14) demonstrated that MALAT1 was also involved in regulating the biological functions of vascular endothelial cells, including phenotypic switching, basal sprouting and migration. However, whether MALATl also serves a critical role in high glucose (HG)-induced H9C2 cardiomyocyte pyroptosis has not been previously reported. In recent years, numerous studies have demonstrated that miR-141-3p is closely associated with DCM development (15,16). In an *in vitro* hypoxia/reoxygenation model, miR-141-3p expression levels were significantly reduced and miR-141-3p overexpression significantly decreased HR-induced cardiomyocyte apoptosis (16). Furthermore, the database prediction indicated that miR-141-3p is one of the downstream targets of MALAT1 (17). However, the roles and mechanisms underlying the lncRNA-MALAT1/miR-141-3p axis in HG-induced cardiomyocyte pyroptosis are not completely understood.

Based on the aforementioned studies, the present study established MALAT1 and miR-141-3p knockdown and overexpression in HG-treated H9C2 cardiomyocytes to investigate whether lncRNA-MALAT1 could target miR-141-3p and regulate HG-induced H9C2 cardiomyocyte pyroptosis. The results of the present study may provide a novel molecular target and research direction for the potential treatment of DCM.

Materials and methods

Cell culture and groups. Rat cardiomyocytes (H9C2; The Cell Bank of Type Culture Collection of The Chinese Academy of Sciences) were cultured in DMEM (HyClone; GE Healthcare Life Sciences) supplemented with 10% fetal bovine serum (FBS; cat. no. S9030; Beijing Solarbio Science & Technology Co., Ltd.) and 1% penicillin-streptomycin in a constant temperature incubator at 37˚C with 5% CO_2. Cells were subcultured every 2-3 days and used for subsequent experiments. According to a previous study (18), cells were divided into the following two groups: i) Normal glucose; cells were incubated with normal glucose (NG; 5.5 mM); and ii) high glucose; cells were incubated with high glucose (HG; 30 mM) at 37˚C until they reached ~70-80% confluence.

Reverse transcription-quantitative PCR (RT-qPCR). RT-qPCR was performed to measure MALAT1 and miR-141-3p expression cells. Cells were centrifuged at 4˚C for 15 min at 850 x g. Total RNA was extracted using TRIzol® (cat. no. N065; Nanjing Jiancheng Bioengineering Institute). The RNA purity was assessed using a spectrophotometer (UV-1600PC; Shanghai Mapada Instruments Co., Ltd.). Subsequently, total RNA was reverse transcribed into cDNA using a PrimeScript™ RT reagent kit (cat. no. RR047A; Takara Bio, Inc.). Subsequently, qPCR was performed using SYBR Green PCR Master Mix (MedChem Express) on a Mastercycler® nexus X2 (Roche Diagnostics) according to the manufacturer's protocol. The following thermocycling conditions were used for qPCR: 95˚C for 15 sec; followed by 35 cycles at 60˚C for 60 sec and 72˚C for 40 sec, then 72˚C for 10 min. The following primers (Shanghai Shenggong Biology Engineering Technology Service, Ltd.) were used for qPCR: MALAT1 forward, 5'-CTT CCCTAGGGGATTTCAGG-3-' and reverse, 5'-GATGCA AATGCCTCTGAGTG-3'; GAPDH forward, 5'-TGACTT CAACAGCGACACCCA-3' and reverse, 5'-CACCCTGTT GCTGTAGGCCAAA-3'; miR-141-3p forward, 5'-CTCAAG GCAACCTACCGAAAAG-3' and reverse, 5'-TATCGGACC CATCACGGAGTGG-3'; U6 forward, 5'-CTCGCTTCGGCA GCACA-3' and reverse, 5'-AACGCTTCACGAATTTGC GT-3'. mRNA expression levels were quantified using the $2^{-\Delta\Delta Cq}$ method (19) and normalized to the internal reference genes U6 and GAPDH, respectively.

Cell transfection and grouping. The pcDNA3.1-MALAT1, MALAT1 siRNA (si-MALAT1) and their corresponding controls were purchased from Shanghai GenePharma Co., Ltd. H9C2 cells ($2x10^5$ cells/ml) were transfected at 37˚C for 24 h with Lipofectamine® 2000 (Invitrogen; Thermo Fisher Scientific, Inc.) as previously described (20). Cells were divided into the following groups: i) NG, cells were cultured in normal glucose (5.5 mM) for 24 h; ii) HG, cells were cultured in high glucose (30 mM) for 24 h; iii) HG + MALAT1 overexpression negative control (NC1), cells were transfected with 50 nM control non-targeting adenovirus vector for 24 h, then cultured in HG medium for 24 h; iv) HG + MALAT1 overexpression (MALAT1), cells were transfected with 50 nM pcDNA3.1-MALAT1 for 24 h, then cultured in HG medium for 24 h; v) HG + MALAT1 siRNA scramble control (NC2) cells were transfected with 50 nM MALAT1 siRNA scramble control (5'-UUCUCCGAACGUGUCACGUTT-3') for 24 h then cultured in HG medium for 24 h; and vi) HG + MALAT1 siRNA (si-MALAT1), cells were transfected with 50 nM MALAT1 siRNA (5'-GATCCATAATCGGTTTCAA-3') for 24 h then cultured in HG medium for 24 h. Transfection efficiency was assessed via RT-qPCR.

Dual luciferase reporter assay. The target gene prediction between lnc MALAT1 and miR-141-3p was performed using TargetScan software 3.0 (www.targetscan.org). Wild-type (WT) and mutant (MUT) 3'-untranslated regions (UTRs) of MALAT1 were cloned into the pGL3/luciferase vector (Promega Corporation). The sequences were inserted downstream of the luciferase gene and cloned as previously described (17). Cells ($2x10^5$ cells/ml) were co-transfected with 50 ng MALAT1 WT 3'UTR or MALAT1 MUT 3'UTR, then co-transfected with 20 nM miR-141-3p mimic (5'-UAA CACUGUCUGGUAAAGAUGG-3') or miR-NC (5'-ACG UGACACGUUCGGAGAATT-3') into H9C2 cells using

Lipofectamine 2000 (Invitrogen; Thermo Fisher Scientific, Inc.). At 48 h post-transfection, luciferase activities were measured using the Dual Luciferase Reporter System (Promega Corporation). Firefly luciferase activity was normalized to Renilla luciferase activity for each transfected cell sample.

Detection of pyroptosis by TUNEL staining. Cells were fixed with 4% paraformaldehyde at room temperature for 30 min and washed with phosphate buffer saline (PBS) three times, 5 min each time. Subsequently, cells were incubated with PBS containing 0.3% Triton X-100 on ice for 5 min at room temperature. Following washing twice with PBS, cells were incubated with 50 μl TUNEL detection solution (Beyotime Institute of Biotechnology) for 1 h at 37˚C in the dark and then washed three times with PBS. Cell nuclei were stained with DAPI (1 mg/ml) at room temperature for 10 min in the dark. After washing with PBS, the plate was sealed with anti-fluorescence quenching liquid and observed using a BX51 fluorescence microscope (Olympus Corporation). A total of five fields were viewed under x400 magnification. The TUNEL positive cell rate (%) was calculated according to the following formula: (Number of positive cells/total number of cells) x100.

Immunofluorescence staining. GSDMD-N expression was detected by performing immunofluorescence staining. Cells ($2x10^4$ cells/ml) were seeded on the slide fixed with 4% paraformaldehyde at room temperature for 30 min and washed with PBS three times, 5 min each time. Following drying of the slide using absorbent paper, the slides were blocked with 5% goat serum (MP20008; Yuanye, Shanghai, China) for 30 min at room temperature. The slides were incubated with a rabbit anti-rat GSDMD-N polyclonal primary antibody (1:200; cat. no. AF4013; Affinity Biosciences) at 4˚C for overnight in dark. Subsequently, the slides were incubated at room temperature for 1 h, washed four times with PBS and incubated with 50 μl FITC-labeled goat anti-rabbit IgG secondary antibody (1:500, cat. no. bs-0295G; BIOSS) for 1 h at room temperature in dark. Following washing, cells were counterstained with DAPI (1 mg/ml) at room temperature for 10 min in dark. Anti-fluorescence quenching liquid was used for sealing. Stained cells were observed using a fluorescent microscope (BX51; Olympus Corporation). A total of five fields were viewed under 400 magnification.

Western blotting. The protein expression levels of ASC, GSDMD-N, caspase-1, NLRP3 and GSDMD were measured via western blotting. Cells were lysed using ice-cold RIPA lysis buffer (Beyotime Institute of Biotechnology) and centrifuged at 850 x g for 20 min at 4˚C to obtain the supernatant. Protein concentrations were determined using a BCA kit (cat. no. A045-4-2; Nanjing Jiancheng Bioengineering Institute). Proteins (40 μg) were separated via 10% SDS-PAGE and transferred to PVDF membranes (cat. no. 3010040001; Roche Diagnostics) for 30 min. Following blocking in tris-buffered saline containing 2% Tween-20 (TBST) solution supplemented with 5% BSA (Beijing Solarbio Science & Technology Co., Ltd.) for 1 h at 4˚C, the membranes were incubated overnight at 4˚C with primary antibodies (diluted in TBST supplemented with 3% BSA) targeted against the following: ASC (1:1,000; cat. no. DF7540; Affinity Biosciences), GSDMD-N (1:500; cat. no. AF4013; Affinity Biosciences), caspase-1 (1:1,000; cat. no. ET1608-69; HUABIO), NLRP3 (1:500; cat. no. ab91413; Abcam), GSDMD (1:500; cat. no. ab245565; Abcam) and β-actin (1:1,000; cat. no. ET1702-67; HUABIO). Subsequently, the membranes were incubated with a HRP-conjugated goat anti-rabbit IgG secondary antibody (1:2,000; cat. no. bs-0295G; BIOSS) for 1 h at room temperature. Following washing with PBS, protein bands were visualized by incubating the membranes with ECL developer (Thermo Fisher Scientific, Inc.) in the dark, followed by detection using the Gel Doc XR System gel imaging analysis system (Bio-Rad Laboratories, Inc.). Protein expression levels were semi-quantified using ImageJ software 5.0 (National Institutes of Health) with β-actin as the loading control.

Verification experiment. The miR-141-3p siRNA, miR-141-3p mimic, and their corresponding controls were purchased from Shanghai GenePharma Co., Ltd. Cells ($2x10^5$ cells/ml) were transfected with Lipofectamine® 2000 (Invitrogen; Thermo Fisher Scientific, Inc.) and divided into the following groups: i) NG; ii) HG; iii) HG + MALAT1 overexpression; iv) HG + miR-141-3p siRNA scramble control (NC3), cells were transfected with 10 nM miR-141-3p siRNA scramble control (5'-ACGUGACACGUUCGGAGAATT-3') at 37˚C for 24 h, according to previous study (21), then cultured in HG medium for 24 h; v) HG + miR-141-3p siRNA (si-miR), cells were transfected with 10 nM miR-141-3p siRNA (5'-CCA UCUUUACCAGACAGUGUUA-3') at 37˚C for 24 h, then cultured in HG medium for 24 h; vi) HG + MALAT1 overexpression + miR-141-3p overexpression scramble control (MALAT1 + NC4), cells were transfected with 10 nM miR-141-3p mimic scramble control (5'-ACGUGACAC GUUCGGAGAATT-3') and 50 nM pcDNA3.1-MALAT1 at 37˚C for 24 h, then cultured in HG medium for 24 h; and vii) HG + MALAT1 overexpression + miR-141-3p overexpression (MALAT1 + miR), cells were transfected with 10 nM miR-141-3p mimic (5'-UAACACUGUCUGGUA AAGAUGG-3') and 50 nM pcDNA3.1-MALAT1 at 37˚C for 24 h, then cultured in HG medium for 24 h. Transfection efficiency was determined via RT-qPCR.

Statistical analysis. Statistical analyses were performed using SPSS software (version 19.0; IBM Corp.). A total of three experimental repeats were performed and data are presented as the mean ± SD. Comparisons among multiple groups were analyzed using one-way ANOVA followed by Tukey's post hoc test. $P<0.05$ was considered to indicate a statistically significant difference.

Results

MALAT1 and miR-141-3p expression levels in H9C2 cells. MALAT1 mRNA expression levels were significantly increased, whereas miR-141-3p expression levels were markedly decreased in the HG group compared with the NG group (Fig. 1A and B). In the MALAT1 group, MALAT1 mRNA expression levels were notably increased, whereas miR-141-3p expression levels were significantly decreased compared with the HG group (Fig. 1C and D). The opposite

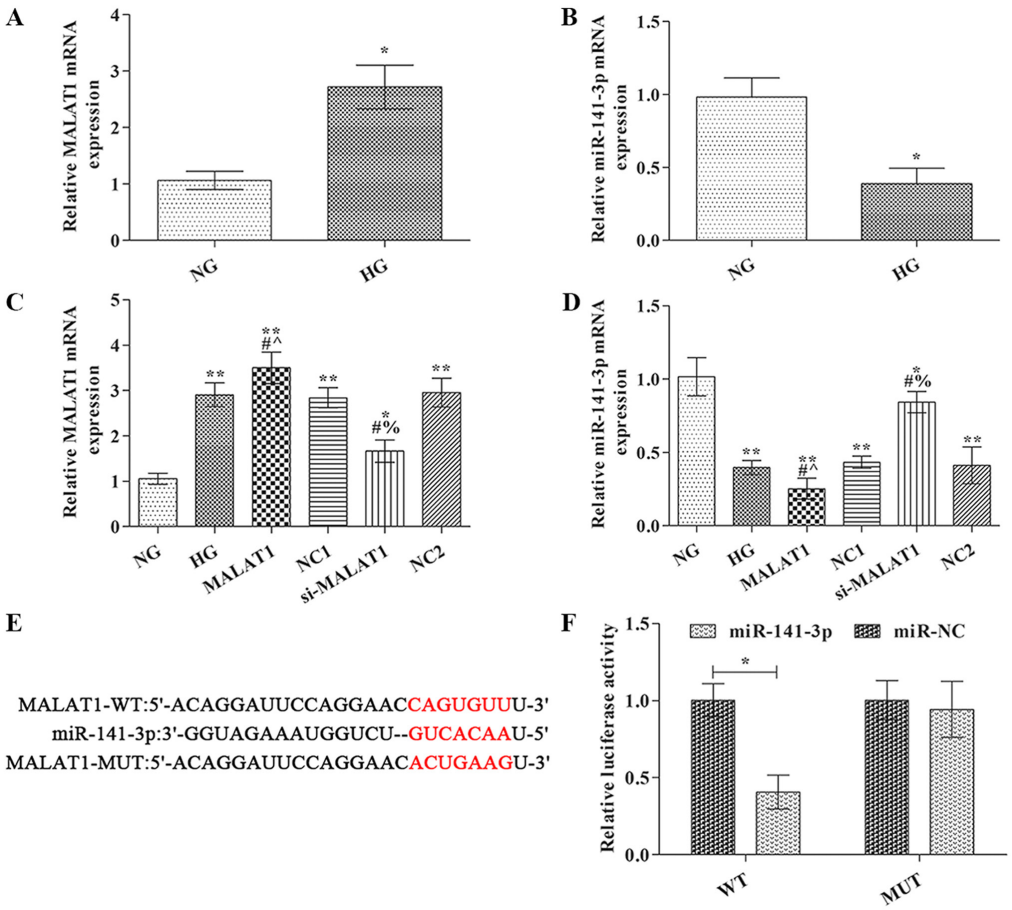

Figure 1. MALAT1 and miR-141-3p expression levels were detected via reverse transcription-quantitative PCR. (A) MALAT1 and (B) miR-141-3p expression levels. (C) Transfection efficiency of MALAT1 overexpression and knockdown. (D) Effect of MALAT1 knockdown and overexpression on miR-141-3p expression. (E) TargetScan was used to predict the binding site between miR-141-3p and MALAT1. (F) Dual luciferase reporter assays were conducted to verify the interaction between miR-141-3p and MALAT1. *P<0.05 and **P<0.01 vs. NG; $^{\#}$P<0.05 vs. HG; $^{\wedge}$P<0.05 vs. NC1; $^{\%}$P<0.05 vs. NC2. MALAT1, metastasis-associated lung adenocarcinoma transcript-1; miR, microRNA; NG, normal glucose; HG, high glucose; NC, negative control; NC1, MALAT1 overexpression NC group; NC2, MALAT1 knockdown NC group; WT, wild-type; MUT, mutant; si, small interfering RNA.

effects on MALAT1 and miR-141-3p expression levels were observed in the si-MALAT1 group compared with the HG group.

MALAT1 was identified as a target of miR-141-3p using TargetScan (www.targetscan.org) (Fig. 1E). To further verify whether miR-141-3p targeted MALAT1, a dual luciferase reporter system was used (Fig. 1F). The results indicated that compared with miR-NC, miR-141-3p mimic significantly reduced the luciferase activity of MALAT1 WT 3'UTR, but did not significantly alter the luciferase activity of MALAT1 MUT 3'UTR.

Effects of MALAT1 on cell pyroptosis and GSDMD-N expression. Blue staining indicated a standard cell nucleus, whereas green staining indicated a TUNEL label-positive nucleus (Fig. 2A). Pyroptosis was not observed in the NG group. The rate of TUNEL positive cells in the HG group was markedly higher compared with the NG group (P<0.05). Compared with the HG group, the rate of TUNEL positive cells was significantly increased in the MALAT1 group, but significantly reduced in the si-MALAT1 group (P<0.05). GSDMD-N expression in the NG group was notably lower compared with the HG group, with protein expression localized on the cell membrane (P<0.01; Fig. 2B). Compared with the HG group, GSDMD-N expression was significantly increased in the MALAT1 group, but significantly decreased in the si-MALAT1 group (P<0.01).

Effect of MALAT1 on pyroptosis-associated protein expression levels. Compared with the NG group, ASC, GSDMD-N, caspase-1 and NLRP3 protein expression levels were significantly increased, but GSDMD protein expression levels were significantly decreased in the HG group (all P<0.05; Fig. 3). Compared with the HG group, ASC, GSDMD-N, caspase-1 and NLRP3 protein expression levels were significantly increased, whereas GSDMD protein expression levels were significantly decreased in the MALAT1 group (all P<0.05). However, the opposite effects on protein expression were observed in the si-MALAT1 group compared with the HG group (all P<0.05).

Effects of MALAT1 on miR-141-3p expression, cell pyroptosis and GSDMD-N expression. To assess the transfection efficiency of miR-141-3p mimic and inhibitor, the expression levels of miR-141-3p were analyzed via RT-qPCR (Fig. 4A). Compared with the NG group, miR-141-3p expression was significantly increased by miR-141-3p mimic and decreased by miR-141-3p siRNA (P<0.01). Furthermore, cells were transfected with

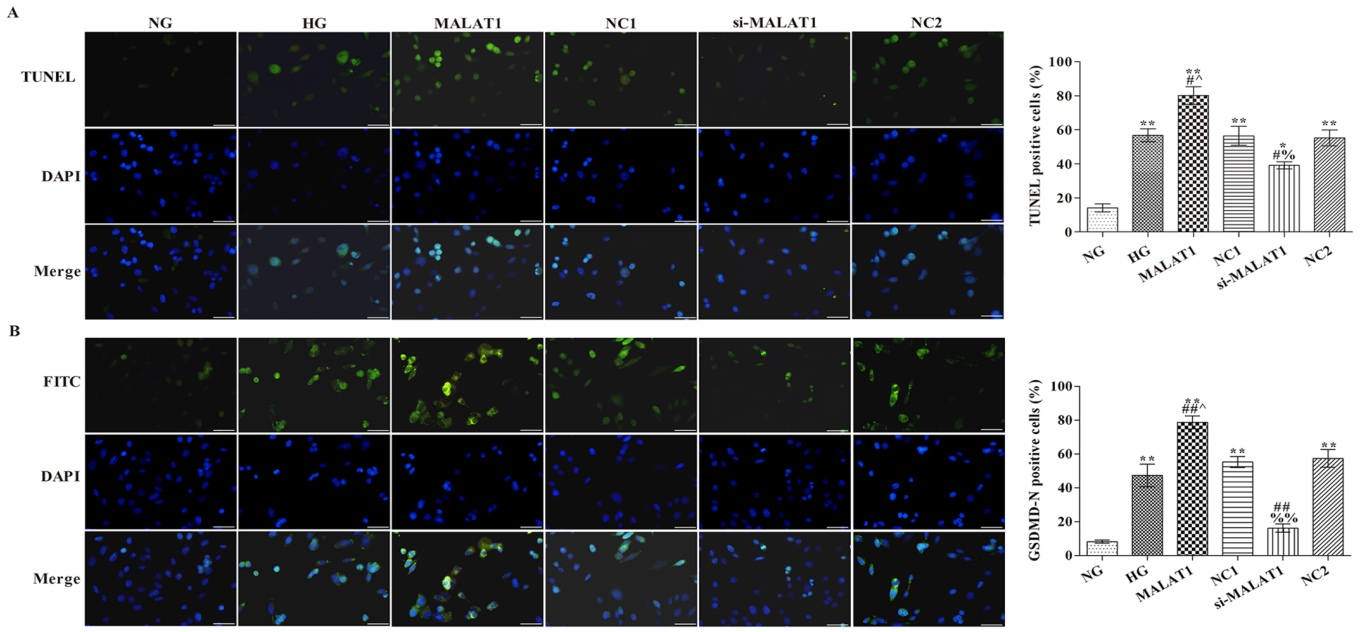

Figure 2. Effects of MALAT1 on cell pyroptosis and GSDMD-N expression. (A) TUNEL staining was performed to detect the levels of pyroptosis (scale bar, 50 μm). (B) GSDMD-N expression levels were detected via immunofluorescence staining (scale bar, 50 μm). *P<0.05 and **P<0.01 vs. NG; $^{\#}$P<0.05 and $^{\#\#}$P<0.01 vs. HG; $^{\wedge}$P<0.05 vs. NC1; $^{\%}$P<0.05, $^{\%\%}$P<0.01 vs. NC2. MALAT1, metastasis-associated lung adenocarcinoma transcript-1; GSDMD, gasdermin D; NG, normal glucose; HG, high glucose; NC, negative control; NC1, MALAT1 overexpression NC group; NC2, MALAT1 knockdown NC group; si, small interfering RNA.

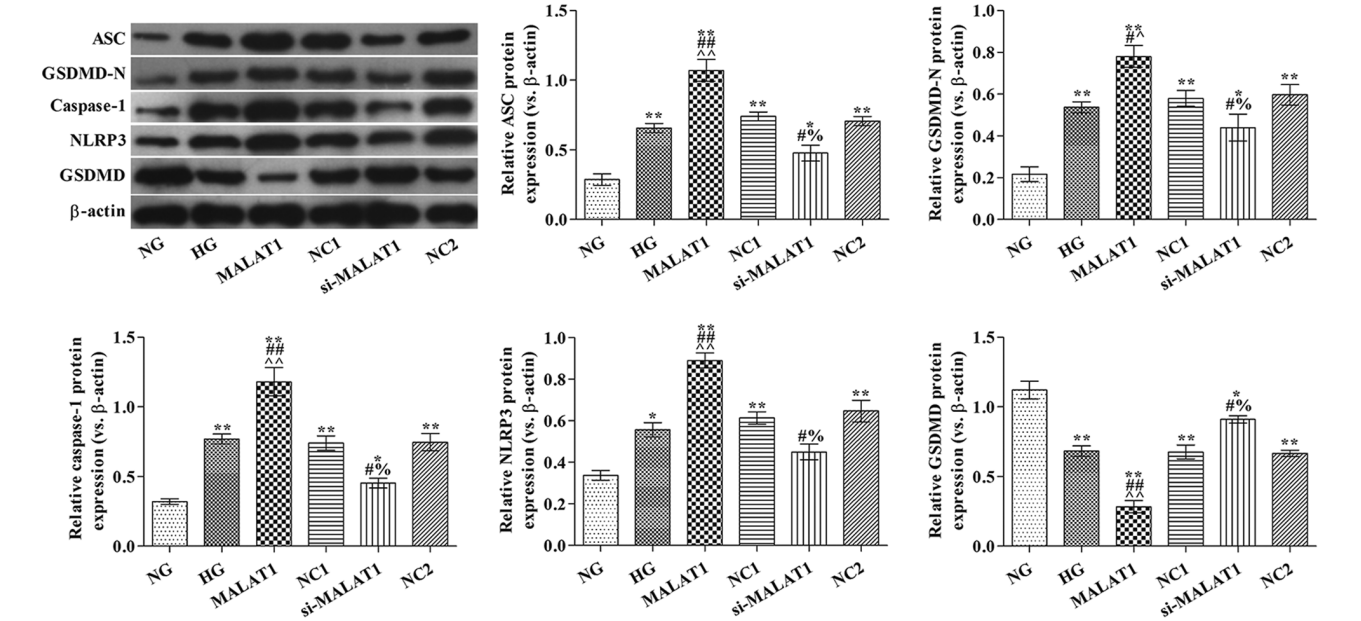

Figure 3. Effects of MALAT1 on pyroptosis-associated protein expression levels. ASC, GSDMD-N, caspase-1, NLRP3 and GSDMD protein expression levels were measured via western blotting. *P<0.05 and **P<0.01 vs. NG; $^{\#}$P<0.05 and $^{\#\#}$P<0.01 vs. HG; $^{\wedge}$P<0.05 and $^{\wedge\wedge}$P<0.01 vs. NC1; $^{\%}$P<0.05 vs. NC2. MALAT1, metastasis-associated lung adenocarcinoma transcript-1; ASC, apoptosis-associated speck-like protein; GSDMD, gasdermin D; NLRP3, nucleotide oligomerization domain-like receptor protein 3; NG, normal glucose; HG, high glucose; NC, negative control; NC1, MALAT1 overexpression NC group; NC2, MALAT1 knockdown NC group; si, small interfering RNA.

MALAT1 mimic (Fig. 4B). miR-141-3p expression levels in all other groups were significantly reduced compared with the NG group (Fig. 4B). Compared with the HG group, miR-141-3p knockdown or MALAT1 overexpression significantly decreased miR-142-3p expression (both P<0.05). Compared with the MALAT1 group, miR-142-3p expression was significantly increased in the MALAT1 + miR group (P<0.05). GSDMD-N expression levels were significantly increased in all other groups compared with the NG group (all P<0.01; Fig. 4D). The rate of TUNEL positive cells (all P<0.05; Fig. 4C) and GSDMD-N expression levels (all P<0.01; Fig. 4D) were significantly increased in the MALAT1, si-miR and MALAT1 + NC4 groups compared with the HG group. In addition, the number of TUNEL positive cells and GSDMD-N expression levels

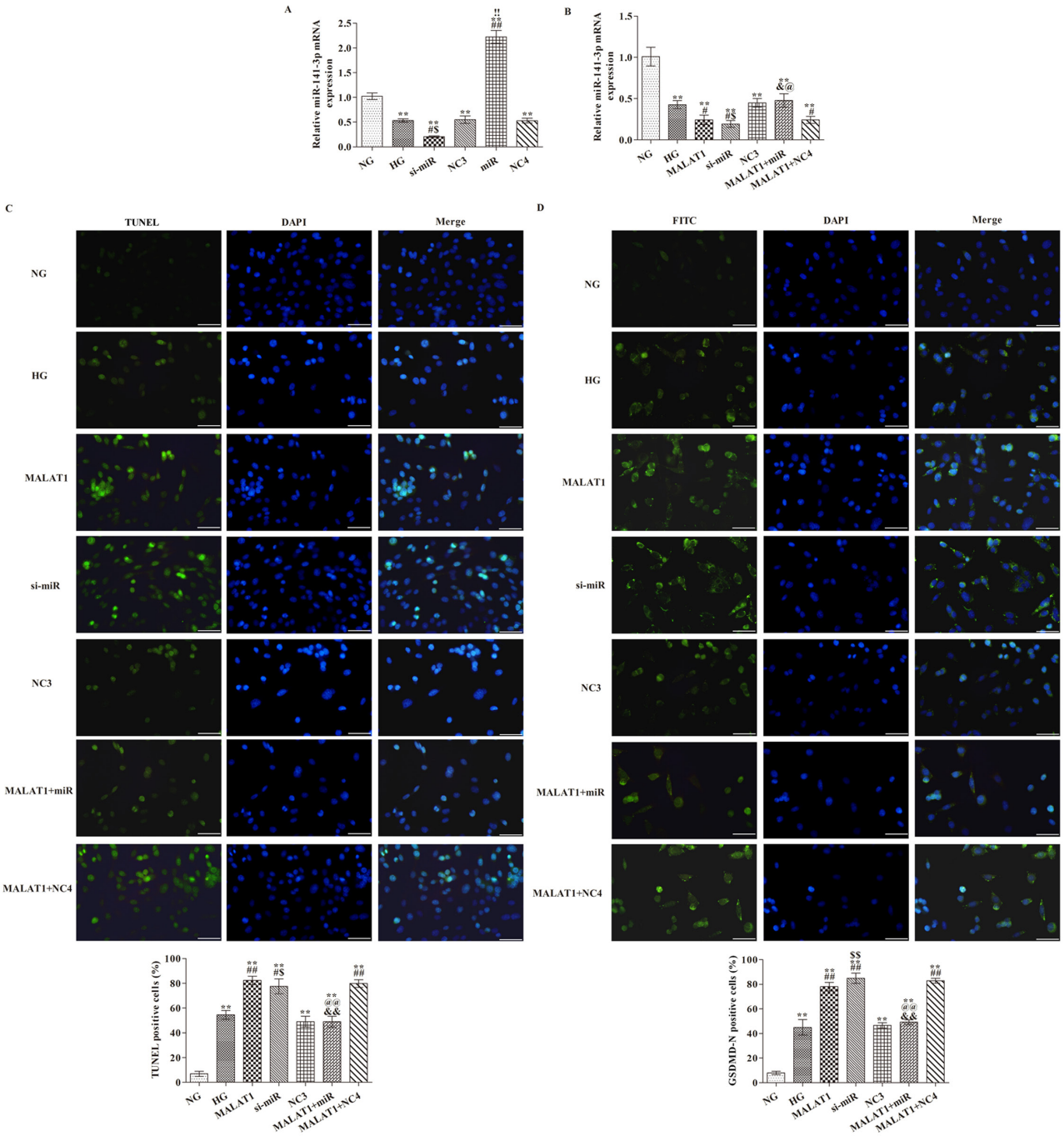

Figure 4. Effects of MALAT1 on cell pyroptosis and GSDMD-N expression are mediated via targeting miR-141-3p. (A) Transfection efficiency of miR-141-3p overexpression and knockdown. (B) Effect of miR-141-3p overexpression and knockdown on miR-141-3p expression levels following HG treatment. (C) TUNEL staining was performed to detect the levels of pyroptosis (scale bar, 50 μm). (D) GSDMD-N expression levels were detected via immunofluorescence staining (scale bar, 50 μm). **P<0.05 vs. NG; $^{\#}$P<0.05 and $^{\#\#}$P<0.01 vs. HG; $^{\&}$P<0.05 and $^{\&\&}$P<0.01 vs. MALAT1; $^{\$}$P<0.05 and $^{\$\$}$P<0.01 vs. NC3; $^{!!}$P<0.01 vs. NC4; $^{@}$P<0.05 and $^{@@}$P<0.01 vs. MALAT1 + NC4. MALAT1, metastasis-associated lung adenocarcinoma transcript-1; GSDMD, gasdermin D; miR, microRNA; HG, high glucose; NG, normal glucose; NC, negative control; NC3, miR-141-3p knockdown NC group; NC4, miR-141-3p overexpression NC group; si, small interfering RNA. The cell nuclei were stained with DAPI; The positive nucleus were stained with FITC.

were also significantly reduced in the MALAT1 + miR group compared with the MALAT1 group (both P<0.01).

MALAT1 alters pyroptosis-related protein expression levels via targeting miR-141-3p. ASC, GSDMD-N, caspase-1 and NLRP3 protein expression levels were significantly increased in all other groups, whereas GSDMD protein expression levels were significantly decreased in all other groups compared with the NG group (all P<0.05; Fig. 5). ASC, GSDMD-N, caspase-1 and NLRP3 protein expression levels in the MALAT1, si-miR and MALAT1 + NC4 groups were significantly increased, whereas GSDMD protein expression levels were significantly decreased compared with the HG group (all P<0.05). ASC, GSDMD-N, caspase-1 and NLRP3 protein expression levels in the MALAT1 + miR group were significantly reduced, whereas GSDMD protein expression levels were significantly increased compared with the MALAT1 group (all P<0.05).

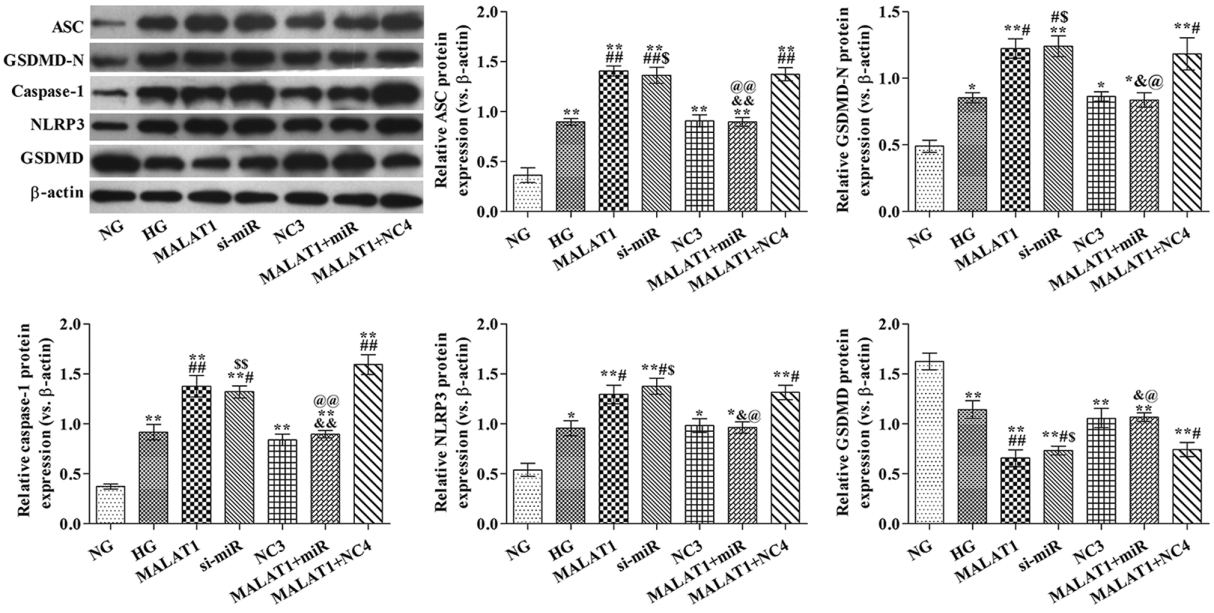

Figure 5. Effects of MALAT1 on pyroptosis-associated protein expression levels are mediated via targeting miR-141-3p. ASC, GSDMD-N, caspase-1, NLRP3 and GSDMD protein expression levels were measured via western blotting. *P<0.05 and **P<0.05 vs. NG; $^{\#}$P<0.05 and $^{\#\#}$P<0.05 vs. HG; $^{\&}$P<0.05 and $^{\&\&}$P<0.01 vs. MALAT1; $^{\$}$P<0.05 and $^{\$\$}$P<0.05 vs. NC3; $^{@}$P<0.05 and $^{@@}$P<0.01 vs. MALAT1 + NC4. MALAT1, metastasis-associated lung adenocarcinoma transcript-1; miR, microRNA; ASC, apoptosis-associated speck-like protein; GSDMD, gasdermin D; NLRP3, nucleotide oligomerization domain-like receptor protein 3; NG, normal glucose; HG, high glucose; NC, negative control; NC3, miR-141-3p knockdown NC group; NC4, miR-141-3p overexpression NC group; si, small interfering RNA.

Discussion

The development of diabetic myocardial damage is a complex process; although, hyperglycemia is typically considered as the primary risk factor leading to diabetic myocardial damage (22), the specific molecular mechanism that induces cell damage is not completely understood. A previous study indicated that pyroptosis was closely associated with the occurrence and development of DCM (23). In addition, caspase-1 mRNA and protein expression levels were significantly increased in the cardiomyocytes of diabetic model rats (24). An additional study demonstrated that NLRP3 activated caspase-1-mediated pyroptosis in DCM and served a significant role in the development of the disease (25). Therefore, the molecular mechanism underlying HG-induced cardiomyocyte pyroptosis could be used to identify novel molecular therapeutic targets for DCM. In the present study, pyroptosis-associated protein expression levels, including ASC, GSDMD-N, caspase-1, NLRP3 and GSDMD, were assessed in NG- and HG-treated cells. The results demonstrated that pyroptosis-associated protein expression levels were significantly increased in the HG group compared with the NG group, which suggested that HG induced H9C2 cardiomyocyte pyroptosis.

In addition, lncRNAs interact with miRNAs, which influences the development of several diseases, including DCM (12,26). In a previous study, the involvement of MALAT1 in DCM was examined, and the results indicated that MALAT1 participated in the regulation of cardiomyocyte apoptosis (12). Gong *et al* (17) demonstrated that lncRNA MALAT1 bound to miR-141-3p, which decreased miR-141-3p expression levels during the development of atherosclerosis. Therefore, the present study explored the effect of lncRNA-MALAT1 on HG-induced H9C2 cardiomyocyte pyroptosis. The results suggested that the effects of MALAT1 were mediated via targeting miR-141-3p. MALAT1 expression levels were significantly increased, whereas miR-141-3p expression levels were significantly decreased in HG-treated H9C2 cells compared with the NG group. Furthermore, compared with the HG group, MALAT1 overexpression significantly reduced miR-141-3p expression levels, increased the rate of TUNEL positive cells and upregulated pyroptosis-associated protein expression levels, whereas MALAT1 knockdown displayed the opposite effects. Moreover, the rate of TUNEL positive cells, and the expression levels of GSDMD-N and pyroptosis-associated proteins were all significantly reduced by miR-141-3p overexpression in MALAT1-overexpression H9C2 cells.

At present, >100,000 lncRNAs have been identified in the human body (27). However, despite the vast number of lncRNAs and their complex regulatory networks, the functions of the majority of lncRNAs are not completely understood, which includes lncRNAs involved in the regulation of glucose and the pathogenesis of diabetes. In the present study, there were several limitations. MALAT1 and miR-141-3p in rats with diabetic cardiomyopathy needs further exploration, as do mechanisms of MALAT1 and miR-141-3p. Collectively, the present study provided novel insight for the diagnosis and targeted therapy of DCM. The results suggested that it might be possible to prevent the damage caused by HG-induced pyroptosis in the early stages, thereby preventing the occurrence and development of DCM.

Acknowledgements

Not applicable.

Funding

No funding was received.

Availability of data and materials

The datasets used and/or analyzed during the current study are available from the corresponding author on reasonable request.

Authors' contributions

AW and WS designed the study, performed the experiments, collected data and drafted the manuscript. WS and FM analyzed and interpreted the experimental data. AW and FM assessed the raw data and were responsible for confirming the legitimacy of the data. FM participated in the coordination of the study and revised the manuscript. All authors read and approved the final manuscript.

Ethics approval and consent to participate

Not applicable.

Patient consent for publication

Not applicable.

Competing interests

The authors declare that they have no competing interests.

References

1. Lee WS and Kim J: Diabetic cardiomyopathy: Where we are and where we are going. Korean J Intern Med 32: 404-421, 2017.
2. Shen L, Li L, Li M, Wang W, Yin W, Liu W and Hu Y: Silencing of NOD2 protects against diabetic cardiomyopathy in a murine diabetes model. Int J Mol Med 42: 3017-3026, 2018.
3. Wakisaka M, Kamouchi M and Kitazono T: Lessons from the trials for the desirable effects of sodium glucose Co-transporter 2 inhibitors on diabetic cardiovascular events and renal dysfunction. Int J Mol Sci 20: 5668, 2019.
4. Hu X, Bai T, Xu Z, Liu Q, Zheng Y and Cai L: Pathophysiological fundamentals of diabetic cardiomyopathy. Compr Physiol 7: 693-711, 2017.
5. American, Diabetes, Association: 2. Classification and diagnosis of diabetes: Standards of medical care in diabetes-2019. Diabetes Care 42(Suppl 1): S13-S28, 2019.
6. Pasparakis M and Vandenabeele P: Necroptosis and its role in inflammation. Nature 517: 311-320, 2015.
7. Xu B, Jiang M, Chu Y, Wang W, Chen D, Li X, Zhang Z, Zhang D, Fan D, Nie Y, *et al*: Gasdermin D plays a key role as a pyroptosis executor of non-alcoholic steatohepatitis in humans and mice. J Hepatol 68: 773-782, 2018.
8. Shi J, Gao W and Shao F: Pyroptosis: Gasdermin-mediated programmed necrotic cell death. Trends Biochem Sci 42: 245-254, 2016.
9. Yue RC, Lu SZ, Luo Y, Wang T, Liang H, Zeng J, Liu J and Hu HX: Calpain silencing alleviates myocardial ischemia-reperfusion injury through the NLRP3/ASC/Caspase-1 axis in mice. Life Sci 233: 116631, 2019.
10. Biswas S, Thomas AA and Chakrabarti S: LncRNAs: Proverbial genomic 'Junk' or key epigenetic regulators during cardiac fibrosis in diabetes? Front Cardiovasc Med 5: 28, 2018.
11. Asrih M and Steffens S: Emerging role of epigenetics and miRNA in diabetic cardiomyopathy. Cardiovasc Pathol 22: 117-125, 2013.
12. Zhang M, Gu H, Xu W and Zhou X: Down-regulation of lncRNA MALAT1 reduces cardiomyocyte apoptosis and improves left ventricular function in diabetic rats. Int J Cardiol 203: 214-216, 2016.
13. Ji P, Diederichs S, Wang W, Böing S, Metzger R, Schneider PM, Tidow N, Brandt B, Buerger H, Bulk E, *et al*: MALAT-1, a novel noncoding RNA, and thymosin beta4 predict metastasis and survival in early-stage non-small cell lung cancer. Oncogene 22: 8031-8041, 2003.
14. Michalik KM, You X, Manavski Y, Doddaballapur A, Zörnig M, Braun T, John D, Ponomareva Y, Chen W, Uchida S, *et al*: Long noncoding RNA MALAT1 regulates endothelial cell function and vessel growth. Circ Res 114: 1389-1397, 2014.
15. Qin Q, Cui L, Zhou Z, Zhang Z, Wang Y and Zhou C: Inhibition of microRNA-141-3p reduces hypoxia-induced apoptosis in H9c2 rat cardiomyocytes by activating the RP105-Dependent PI3K/AKT signaling pathway. Med Sci Monit 25: 7016-7025, 2019.
16. Yao B, Wan X, Zheng X, Zhong T, Hu J, Zhou Y, Qin A, Ma Y and Yin D: Critical roles of microRNA-141-3p and CHD8 in hypoxia/reoxygenation-induced cardiomyocyte apoptosis. Cell Biosci 10: 20, 2020.
17. Gong D, Zhao ZW, Zhang Q, Yu XH, Wang G, Zou J, Zheng XL, Zhang DW, Yin WD and Tang CK: The long noncoding RNA metastasis-associated lung adenocarcinoma Transcript-1 Regulates CCDC80 expression by targeting miR-141-3p/miR-200a-3p in vascular smooth muscle cells. J Cardiovasc Pharmacol 75: 336-343, 2020.
18. Zhang J, Jiang T, Liang X, Shu S, Xiang X, Zhang W, Guo T, Xie W, Deng W and Tang X: lncRNA MALAT1 mediated high glucose-induced HK-2 cell epithelial-to-mesenchymal transition and injury. J Physiol Biochem 75: 443-452, 2019.
19. Livak KJ and Schmittgen TD: Analysis of relative gene expression data using real-time quantitative PCR and the 2(-Delta Delta C(T)) method. Methods 25: 402-408, 2001.
20. Ye Y, Zhang F, Chen Q, Huang Z and Li M: LncRNA MALAT1 modified progression of clear cell kidney carcinoma (KIRC) by regulation of miR-194-5p/ACVR2B signaling. Mol Carcinog 58: 279-292, 2019.
21. Xing Y, Jing H, Zhang Y, Suo J and Qian M: MicroRNA-141-3p affected proliferation, chemosensitivity, migration and invasion of colorectal cancer cells by targeting EGFR. Int J Biochem Cell Biol 118: 105643, 2020.
22. Adameova A and Dhalla NS: Role of microangiopathy in diabetic cardiomyopathy. Heart Fail Rev 19: 25-33, 2014.
23. Luo B, Li B, Wang W, Liu X, Liu X, Xia Y, Zhang C, Zhang Y, Zhang M and An F: Rosuvastatin alleviates diabetic cardiomyopathy by inhibiting NLRP3 inflammasome and MAPK pathways in a type 2 diabetes rat model. Cardiovasc Drugs Ther 28: 33-43, 2014.
24. Shi J, Zhao Y, Wang K, Shi X, Wang Y, Huang H, Zhuang Y, Cai T, Wang F and Shao F: Cleavage of GSDMD by inflammatory caspases determines pyroptotic cell death. Nature 526: 660-665, 2015.
25. Fann DY, Lee SY, Manzanero S, Tang SC, Gelderblom M, Chunduri P, Bernreuther C, Glatzel M, Cheng YL, Thundyil J, *et al*: Intravenous immunoglobulin suppresses NLRP1 and NLRP3 inflammasome-mediated neuronal death in ischemic stroke. Cell Death Dis 4: e790, 2013.
26. Feng Y, Xu W, Zhang W, Wang W, Liu T and Zhou X: LncRNA DCRF regulates cardiomyocyte autophagy by targeting miR-551b-5p in diabetic cardiomyopathy. Theranostics 9: 4558-4566, 2019.
27. Taylor DH, Chu ET, Spektor R and Soloway PD: Long non-coding RNA regulation of reproduction and development. Mol Reprod Dev 82: 932-956, 2015.